A Rapid Scan Internal Reflection Spectroscopic System

Teruo HINOUE, Satoshi OKAZAKI, and Taitiro FUJINAGA

A rapid scan internal reflection spectroscopic system has been developed using an optically transparent electrode (OTE) of tin oxide coated glass, a multi-channel photodetector, and a micro-computer. Some basic examinations of the internal reflection cell were investigated in terms of a typical reversible redox system of ferro/ferricyanide. The electrochemical perturbation of the OTE is performed in one of two ways, i. e., a potential step or a linear sweep mode. The reflectivity — potential curves were obtained directly and analyzed in a manner similar to that in polarography. Internal reflection spectra of electrooxidation/reduction products were obtained *in situ* by a multi-channel photodetector, corresponding to the stepwise changes of the potential of the OTE.

INTRODUCTION

In order to evaluate the electrode reaction mechanism by the optical observation of the electro-generated species *in situ*, various spectro-electrochemical methods have been developed.[1,2] An internal reflection (IR) technique provides helpful information about an interfacial phenomenon.[3-5] In the infrared, the IR technique has been widely used for the acquisition of the spectra of thin films or mono-molecular films as an attenuated total reflection technique and has also been applied to the identification of the electro-chemical products.[6,7] In the visible, Hansen *et al.*[8] were the first to employ the technique for the investigation of electrode reactions by the use of an optically transparent electrode (OTE) of tin oxide coated glass. However, the method has not been diffused except by Kuwana and his followeres,[9] because the technique necessitates a specially elavorate optical path and also a highly sensitive photodetector for the observation of faint optical signals from an IR cell.

In the previous paper,[10] the authors have reported an IR cell assembly for the commercial double-beam type spectrophotometer. In this paper, the authors have developed a rapid scan internal reflection spectroscopic system using a multi-channel photodetector and a micro-computer, and report here about its instrumentation and some basic examinations of the IR cell in terms of a typical reversible redox couple of ferro/ferricyanide.

樋上照男, 岡崎 敏, 藤永太一郎 : Department of Chemistry, Faculty of Science, Kyoto University, Sakyo-ku, Kyoto 606.

EXPERIMENTAL

Reagents and Instruments

Reagents: All chemicals used were of analytical reagent grade. Sample solutions were prepared freshly with twice distilled water.

Instruments: A rapid scan internal reflection spectroscopic system is composed of the following three divisions: (1) A single-beam type spectrophotometer with an accessary optical assembly equipped with an IR cell, (2) An optional electrolysis device of a PAR Potentiostat Model 173 with a Digital Coulomb Counter Model 179 and a Nikko Keisoku Potential Sweeper NPS-2, which imposes an electrochemical perturbation on the OTE, and (3) A micro-computer system, Union Giken System 77, which controls a photodetector, and also processes the experimental data.

Figure 1 illustrates a block diagram of the system manufactured by Union Giken Co. Ltd., Osaka, in which "PS" is a DC Power supply for a light source, "LS" of 50W tungsten lamp, "IRC" is an IR cell, and "M" is a monochromator of a diffraction grating. The monochromatic light is detected by a photomultiplier, "PMT" or a multi-channel-photodetector, "MCPD". One of the notable features of this system is the use of the MCPD in order to obtain a dynamic spectrum of the electrode — solution interface. The MCPD consists of a one-dimensional array of 256 pieces photodiodes, and instantaneously offers an IR spectrum for any 92 nm in the visible region, which is processed by a micro processing unit, "MPU" through an analog-to-digital converter "A/D" and then plotted on an X-Y recorder, "R". The PMT is used for the observation of the reflectivity changes at a constant wavelength corresponding to the potential change, which is recorded directly with a National Pen Recorder VP-6431A.
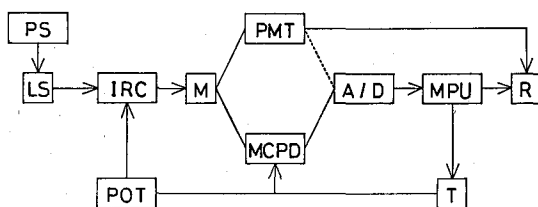

Fig. 1. Block diagram of internal reflection spectroscopic system.
PS: power supply, LS: light source, IRC: IR cell, M: monochromator, PMT: photomultiplier, MCPD: multi-channel photodetector, A/D: analog-to-digital converter, MPU: micro-processing unit, R: X-Y recorder, T: trigger circuit, POT: potentiostat with potential scanner.

The electrochemical perturbation applied to the IR cell is performed in one of two ways, *i. e.*, a potential step mode or a linear sweep mode, which is synchronized with data acquisition through a trigger circuit, "T".

An accessary optical assembly and the IR cell are shown in Figs. 2 and 3, respectively. White light beam radiated from a tungsten lamp, after being collimated and slitted, is incidented to a total reflection plate, "TRP" in the IR cell at an incidence angle of 70° using each pair of mirrors and semi-circular prisms. Thus, the total reflection takes place ten times at the interface between the total reflection plate and the electrolyte solution.
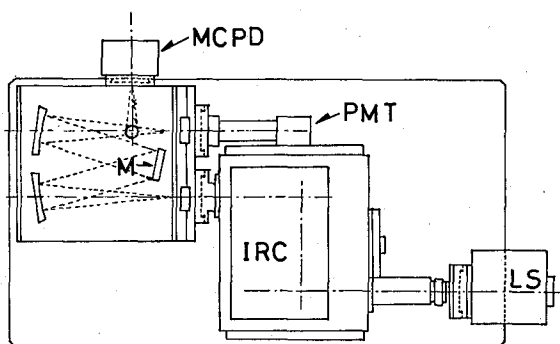
Fig. 2. Scheme of accessary optical assemembly.
LS : light source, IRC : IR cell, M : diffraction grating, PMT :
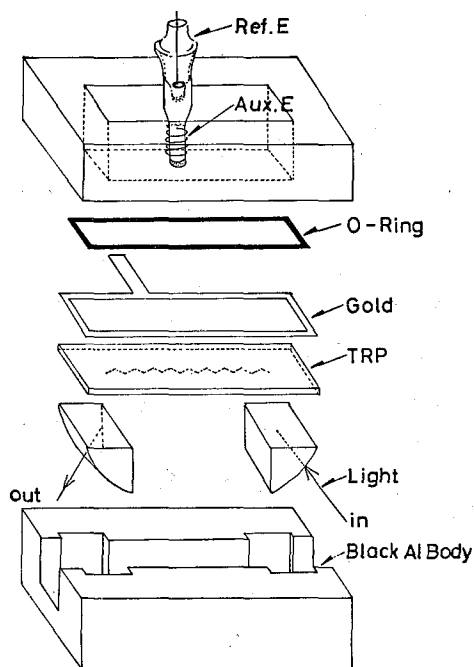photomultiplier, MCPD : multi-channel photodetector.

Fig. 3. Multi-reflection type internal reflection cell.
Ref. E : Ag/AgCl reference electrode, Aux. E : Pt coil counter
electrode, TRP : total reflection plate.

Then the light beam is monochromated by the diffraction grating, and the monochromatic light is detected by the PMT or the MCPD.

Though the IR cell designed here is similar in principle to the one by Kuwana et al.[7-9], the overall arrangement is quite different as seen in Fig. 3, i. e., the total reflection plate is laid at the bottom of the cell, and semi-circular prisms are used. In order to lead the light beam smoothly, small amounts of liquid paraffin are impregnated between the plate and upper planes of the prisms. A gold gasket serves as an electrical lead to the OTE. A cell body is made of black diflon, and the other materials are aluminum with burn black surface. The OTE consists of a quartz glass plate (21×81 mm square

and 1 mm in thickness) coated with tin oxide on the upper surface, which is supplied by Iwaki Glass Co. Ltd.

RESULTS AND DISCUSSION

1) Classical Internal Reflection Spectroscopy

In order to characterize the IR cell used, the classical IR spectra of potassium permanganate were observed, as shown in Fig. 4, using a quartz plate as a total reflection plate over a concentration range from 0.02 M to 0.10 M in 0.32 N sulfuric acid solution. Each spectrum has four absorption maxima at 509, 528, 546, and 568 nm, which correspond to those of a conventional transmission spectrum. Exactly speaking, however, the longer the wavelength becomes, the more the reflection absorbance increases owing to the increase of the path length of the IR cell in proportion to the wavelength, as described in the previous paper.[10] Figure 5 indicates the linear relations between the
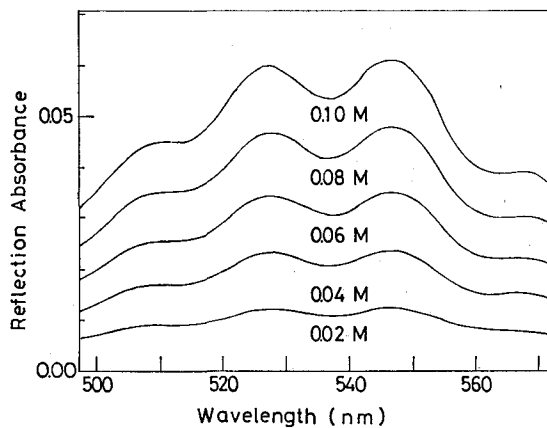

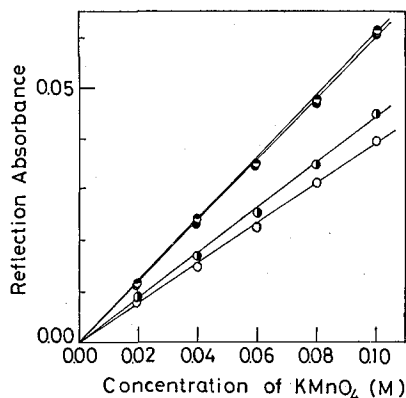Fig. 4. Classical internal reflection spectra of potassium permanganate in 0.32 N sulfuric acid solution.

Fig. 5. Relationships between the reflection absorbance and the concentration for the spectra in Fig. 4.
—◑—: at 509 nm, —●—: 528 nm, —◕—: at 546 nm, —○—: at 568 nm.

reflection absorbance at each maximum and the concentration of permanganate, which verify Beer's law in the IR spectroscopy as given by Eq. (1).[1]

$$A = \varepsilon \cdot n \cdot \delta \cdot C \qquad \qquad \cdots\cdots (1)$$

where, A is the reflection absorbance, ε is the molar extinction coefficient, δ is the path length for the IR cell, n is the number of the total reflections, which was ten times in this work, and C is the concentration of a light absorbing species. The average path length was estimated according to Eq. (1) as 2500 Å at 524 nm per one total reflection.

2) Internal Reflection Spectroscopy Using OTE without electrochemical Perturbation

Figure 6 illustrates the IR spectra of potassium permanganate using a tin oxide coated glass and the MCPD, over the concentration range from 0.02 M to 0.10 M in 0.32 N sulfuric acid solution. Three absorption maxima inherent in permanganate were observed at 528, 546, and 568 nm. However, the absorption maximum at 509 nm was not observed, which was observed in the classical IR spectrum, because the light intensity in this region decreased extremely owing to the interference of the tin oxide layer of the OTE.

Linear relationships between the reflection absorbance at each maximum and the
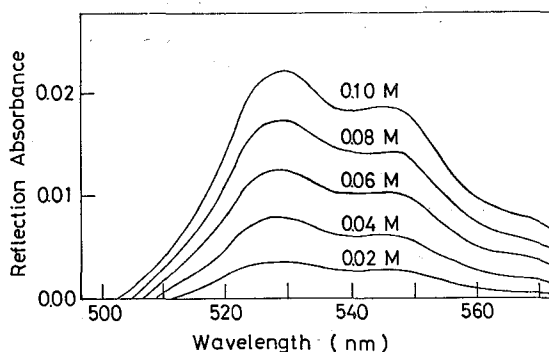

Fig. 6. Internal reflection spectra of potassium permanganate in 0.32 N sulfuric acid solution using OTE as total reflection plate.
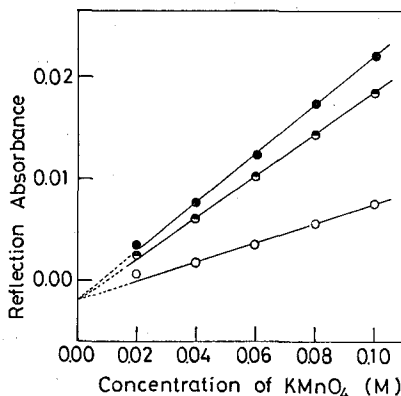

Fig. 7. Relationships between the reflection absorbance and the concentration for the spectra in Fig. 6.
—●—: at 528 nm, —◑—: at 546 nm, —○—: 568 nm.

concentration of permanganate were obtained as shown in Fig. 7, though they did not pass the origin but converged upon one point on the ordinate. Therefore, it is confirmed that OTE cell also satisfies Beer's law defined by Eq. (2) in analogy with in classical IR spectroscopy.[1,9]

$$A = N_{eff} \cdot \varepsilon \cdot n \cdot \delta \cdot C \qquad \cdots\cdots (2)$$

where, N_{eff} is a sensitivity factor characteristic of the type of the OTE.[9,11] The N_{eff} value for the tin oxide coated glass at 524 nm was about 0.36 times that of the classical IR spectroscopy.

3) Application of the Internal Reflection Technique for Monitoring the electrode Process

The parameter δ in Eqs. (1) and (2) means not only the path length in a conventional meaning, but also to the depth of the vertical distance from the electrode surface to the bulk solution. The δ value for this spectroscopy is estimated so small as ca. 2000 Å, that the method is applicable particularly to the optical identification of the electrode reaction products at the vicinity of the electrode surface. The technique was examined in terms of a reversible electrode reaction of ferro/ferricyanide in potassium chloride solution.[12] The changes of the reflectivity at 420 nm were monitored continuously during the anodic or the cathodic potential step. Figure 8 illustrates the anodic oxidation of ferrocyanide ions, where the upward arrows indicate the anodic potential steps from 0.15 V to 0.80 V vs. Ag/AgCl, and the downward arrows show the reverse steps from 0.80 V to 0.15 V. Figure 9 illustrates the cathodic reduction of ferricyanide ions, where the upward arrows show the cathodic steps from 0.80 V to 0.15 V and the downward arrows show the reverse steps.

In the cases of low concentration of the depolarizers, the reflectivities at both steps of the oxidation and reduction attained to the steady-state values within a few seconds. According to Kuwana et al.,[8,9] the behavior of the reflectivity against time at the
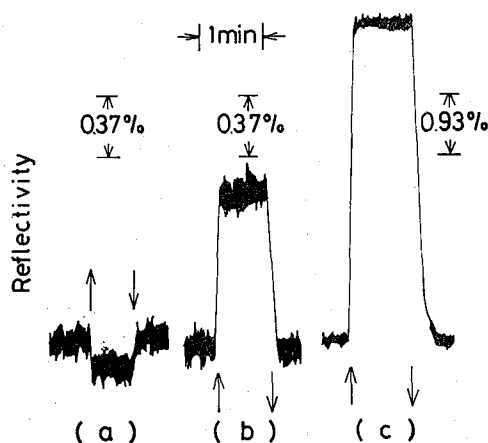

Fig. 8. Potential response of the reflectivity for the oxidation and re-reduction of ferrocyanide in 2.5 M potassium chloride solution.
Concentration of ferrocyanide; (a) : blank, (b) : 20 mM, (c) : 100 mM, wavelength : 420 nm, potential step : 0.15 V → 0.80 V → 0.15 V vs. Ag/AgCl.
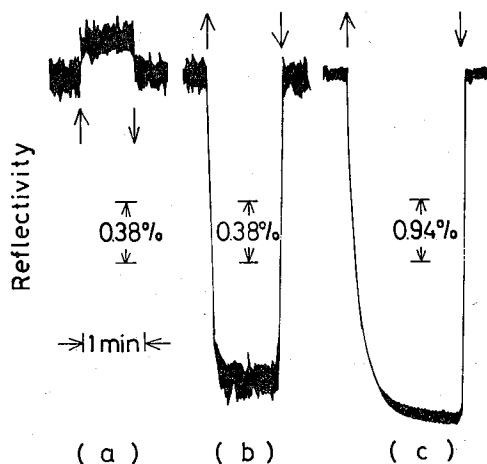
Fig. 9. Potential response of the reflectivity for the reduction and re-oxidation
of ferricyanide in 2.5 M potassium chloride solution.
Concentration of ferricyanide; (a) : blank, (b) : 20 mM, (c) : 100 mM,
wavelength : 420 nm, potential step : 0.80 V → 0.15 V → 0.80 V $vs.$
Ag/AgCl.

chronoamperometric perturbation, $i.$ $e.$, the potential step method, for the reversible
electrode reaction was described as follows: In the case of the colored electrode pro-
duct,*

$$A_{ferri} = \varepsilon_{ferri} \cdot n \cdot b_{eff} \cdot C^{\circ}_{ferro} \cdot (D_{ferro}/D_{ferri})^{1/2}$$
$$\times [1 - \exp(a^2 \cdot t) \cdot \mathrm{erfc}(a \cdot t^{1/2})] \qquad \cdots\cdots (3)$$

Under the condition of t>1 millisecond, Eq. (3) is abbreviated to,

$$A_{ferri} = \varepsilon_{ferri} \cdot n \cdot b_{eff} \cdot C^{\circ}_{ferro} \cdot (D_{ferro}/D_{ferri})^{1/2} \qquad \cdots\cdots (4)$$

where, C° and D have their usual meanings, $b_{eff} = \delta \cdot N_{eff}$, $a = D^{1/2}_{ferri}/\delta$, and t is time after
the potential step. On the other hand, when the depolarizer loses its color, the behavior
is represented in the reverse way as given in Eq. (5),

$$A_{ferri} = \delta_{ferri} \cdot n \cdot b_{eff} \cdot C^{\circ}_{ferri} \cdot \exp(a^2 \cdot t) \cdot \mathrm{erfc}(a \cdot t^{1/2}) \qquad \cdots\cdots (5)$$

Then the change of the reflection absorbance from the initial value is given by Eq. (6)

$$A_{ferri} = A_{final} - A_{initial} = -\varepsilon_{ferri} \cdot n \cdot b_{eff} \cdot C_{ferri} \qquad \cdots\cdots (6)$$

where the minus sign indicates the increase of the reflectivity at the electrode surface
by the electrochemical perturbation. The potential response of the reflectivity in Figs.
8 and 9 agrees with Eqs. (3) and (5), respectively, except that the response time is
considerably longer than that expected from these equations, 1 millisecond. It can be
said that these relaxation effects are attributed to the time lags caused by the slow
potential rise at the electrode surface due to the resistivity of the tin oxide layer of the
OTE, $i.$ $e.$, 200 ohms.

The response behavior of the reflectivity at the reduction of ferricyanide ions was

---

* In these equations, the reflection absorbance is correlated with the reflectivity as follows; under
the condition of $R_o \gg \varDelta R$; $A = \varDelta R/R_o = (1-R)/R_o$, where R and R_o are the reflectivities of colored
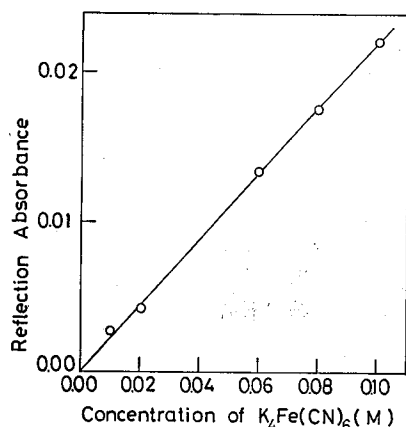and colorless species at the electrode surface, respectively.

Fig. 10. Relationships between the reflection
absorbance and the concentration of
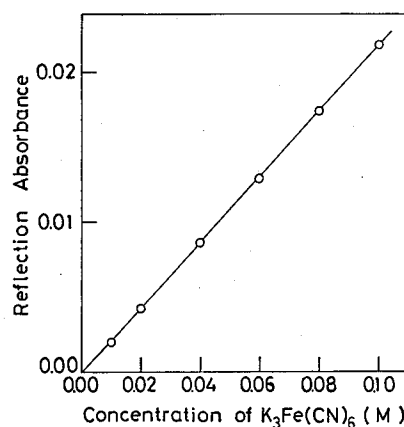ferrocyanide in 2.5 M potassium
chloride solution.

Fig. 11. Relationships between the reflection
absorbance and the concentration of
ferricyanide in 2.5 M potassium
chloride solution.

slower than that of the oxidation of ferrocyanide. This was more significant in the
case of the high concentration of the depolarizer; curves(C) in Figs. 8 and 9. These
phenomena are ascribed simply to the fact that the overpotential at the cathodic step
becomes less and less sufficient owing to the negative shift of the half-wave potential of
ferricyanide, i. e., 0.286 V vs. Ag/AgCl for 40 mM and 0.257 V for 100 mM ferricyanide
(see in Fig. 14), and the cathodic limitation of the accessible potential range of tin oxide
OTE at 0.10 V vs. Ag/AgCl, at which tin oxide is reduced to tin metal.

Figures 10 and 11 show the linear relationships between the concentration of ferro/
ferricyanide ions and their reflection absorbance calculated from the steady-state values
of the reflectivities as expected by Eqs. (4) and (6). Small changes in the reflectivity
were observed even for the blank solutions of 2.5 M potassium chloride by both anodic
and cathodic potential steps as shown in curves (a) in Figs. 8 and 9. These phenomena
are considered to be due to the change of the electric state in the tin oxide layer in
the OTE.[11]

4) Spectro-potentiograms with the Internal Reflection Cell

It is interesting to obtain the dynamic profile of the reflectivity — potential relation on
the basis that the reflection absorbance is corresponding directly to the surface concen-
tration of the depolarizer. Figure 12 illustrates the reflectivity — potential curve of 20 mM
potassium ferrocyanide in 2.5 M potassium chloride solution, which corresponds to a
current — potential curve in polarography. A plot of $\log[(\Delta R)_i - \Delta R]/\Delta R$ vs. E, a wave
analysis in the similar manner as in polarography[13], gives a straight line with a slope of
75 mV and the half-wave potential of 0.336 V vs. Ag/AgCl as shown in Fig. 13. The
limiting reflectivities $(\Delta R)_i$ of spectro-potentiograms for ferro/ferricyanide ions were
proportional directly to their concentration in the manner similar to that in the reflection
absorbance — concentration relationships of Figs. 10 and 11.

From the results of the wave analyses of the spectro-potentiograms of ferro/ferri-
cyanide ions shown in Fig. 14, it is found that their half-wave potentials shift to the more
anodic/or cathodic direction, and their log-plot slopes increase with increasing concentra-
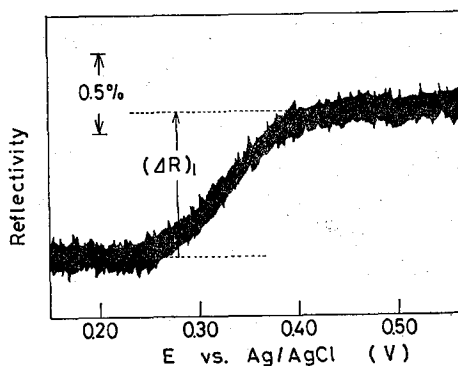
Fig. 12. Reflectivity vs. potential profile for the oxidation of 20 mM potassium ferrocyanide in 2.5 M potassium chloride solution.
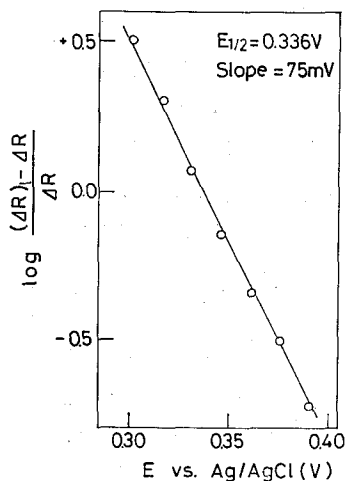

Fig. 13. Plot of log$\{[(\varDelta R)_l - \varDelta R]/\varDelta R\}$ vs. E for the spectro-potentiogram in Fig. 12.

tion of ferro/ferricyanide ions. In the case of the reduction of ferricyanide, the above concentration effects seem to be attributed simply to the ir-drop caused by the increment of the electrolysis current. Therefore, the corrected half-wave potential of ferricyanide, 0.305 V vs. Ag/AgCl obtained by extrapolating the $E_{1/2}$ − C plot to zero concentration of ferricyanide, agrees well with the mean value (0.31 V) of the cathodic (0.35 V) and anodic (0.27 V) peak potentials of the cyclic voltammogram of 1 mM ferrocyanide in 2.5 M potassium chloride solution. And also the corrected log-plot slope, 60 mV suggested that the electrode process of the reduction of ferricyanide ions may be reversible. However, the oxidation process of ferrocyanide ions seems to be rather complicated, even though the effects of ir-drop are corrected, that is, the shift of the half-wave potential is not linear with the concentration of ferrocyanide ions, but becomes very large in the concentration range higher than 60 mM. This result seems to suggest the higher-order association of forrocyanide with potassium cations in the high concentration range of 100 mM: In this study, the concentrations of ferro/ferricyanide were taken to be so high in order to obtain detectable changes in the reflectivity. The major species in the solution
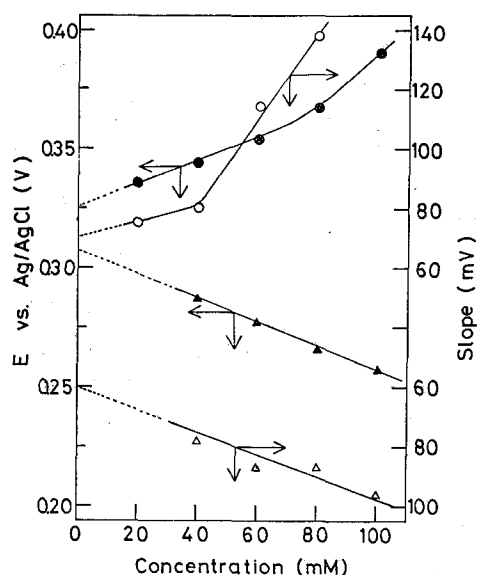
Fig. 14. Dependence of $E_{1/2}$ and log-plot slope on the concentration of the depolarizer.
—●— and —○—: $E_{1/2}$ and slope in the oxidation of ferrocyanide,
—▲— and —△—: those in the reduction of ferricyanide.

seem to be the species associated with at least one potassium cation.[14]

5) Rapid Scan Internal Reflection Spectra of Electrogenerated Species

One of the notable advantages of this system is the use of the MCPD, that is to say, IR spectra of electro-oxidation/reduction products can be observed *in situ*. Figure 15 illustrates the IR spectra of electro-oxidated species of 0.1 M ferrocyanide in 2.5 M potassium chloride solution at various electrode potentials, which are similar to the
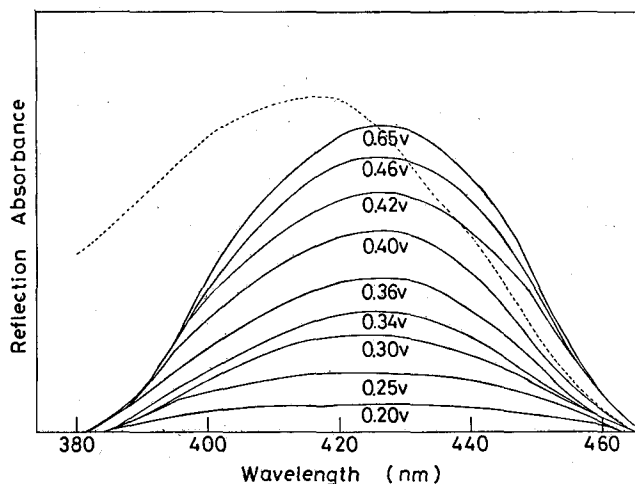

Fig. 15. Rapid scan internal reflection spectra of electrooxidation products of ferrocyanide at various potentials.

conventional transmission spectrum of ferricyanide shown by a dotted line. In general, an IR spectrum cannot be compared directly with the conventional transmission spectrum, because the path length in the IR spectroscopy is proportional to the wavelength, and moreover N_{eff} cannot be estimated exactly.[15] However, it can be said that the path length is compensated relatively, and the N_{eff} value is assumed to be constant in the experimental region of the wavelength, judging from the fact that any interference pattern due to the tin oxide layer is not observed in this region.[15] The half-wave potential and the log-plot slope obtained from the wave-analysis at any wavelength agree with those obtained from the spectro–potentiogram in the same concentration, 100 mM of ferrocyanide solution.

This rapid scan internal reflection spectroscopic system is going to be improved in sensitivity by the use of more effective computer techniques and will be presented elsewhere.

ACKNOWLEDGMENT

REFERENCES

(1) "Advances in Electrochemical Engineering and Electrochemistry", Vol. 9, ed by P. Delahey and C. W. Tobias, John Wiley & Sons, New York, 1973.
(2) W. R. Heineman, *Anal. Chem.*, **50**, 390A (1978).
(3) J. Fahrenfort, *Spectrochim. Acta*, **17**, 698 (1961).
(4) W. N. Hansen, *Spectrochim. Acta*, **21**, 815 (1964).
(5) N. J. Harrik, "Internal Reflection Spectroscopy", Interscience, New York, 1967.
(6) H. B. Mark, Jr. and B. P. Pons, *Anal. Chem.*, **38**, 119 (1966).
(7) D. E. Tallant and D. H. Evans, *Anal. Chem.*, **41** 835 (1969).
(8) W. N. Hansen, T. Kuwana, and R. A. Osteryoung, *J. Amer. Chem. Soc.*, **88**, 1062 (1966).
(9) T. Kuwana, "Electroanalytical Chemistry", Vol. 7, ed by A. J. Bard, Marcel Dekker, Inc., New York, 1974, pp. 1–78
(10) T. Fujinaga, T. Kuwamoto, and T. Hinoue, *Bull. Inst. Chem. Res., Kyoto Univ.*, **54**, 291 (1976).
(11) N. Winograd and T. Kuwana, *J. Electroanal. Chem.*, **23**, 333 (1969).
(12) J. W. Strojek and T. Kuwana, *J. Electroanal. Chem.*, **16**, 471 (1968).
(13) J. Heyrovsky and J. Kuta, "Principles of Polarography", Academic Press, New York, 1966, p. 129.
(14) Stephen R. Cohen and Robert A. Plane, *J. Phys. Chem.*, **61**, 1096 (1957).
(15) V. S. Srinivasen and T. Kuwana, *J. Phys. Chem.*, **72**, 1144 (1968).